IEEE Access
Multidisciplinary | Rapid Review | Open Access Journal

Received September 6, 2020, accepted September 25, 2020, date of publication October 12, 2020, date of current version October 21, 2020.

Digital Object Identifier 10.1109/ACCESS.2020.3030158

Time-Varying Asymmetric Barrier Lyapunov Function-Based Impact Angle Control Guidance Law With Field-of-View Constraint

JIAYI TIAN[1,2], XIBIN BAI[2], HUABO YANG[2], AND SHIFENG ZHANG[2]
[1]China Aerodynamics Research and Development Center, Mianyang 621000, China
[2]College of Aerospace Science and Engineering, National University of Defense Technology, Changsha 410073, China

Corresponding author: Shifeng Zhang (zhang_shifeng@hotmail.com)

ABSTRACT A prerequisite for implementing precision strike is to keep the target locked within the seeker's field-of-view (FOV). To address this constraint, a novel impact angle control guidance law based on the dynamic surface control and time-varying asymmetric Barrier Lyapunov Function is proposed. The FOV constraint, in this article, is equally transformed to a time-varying asymmetric limitation on the missile-target relative velocity perpendicular to the line-of-sight (LOS). Under the proposed guidance law, the velocity component is prevented from overstepping its limitation and eventually approaches zero, thus satisfying the homing requirement and the FOV constraint in an integrated manner. Compared to previous studies, the proposed guidance law does not require the target information and is applicable against moving targets. Also, the proposed guidance law does not use any switching logic, and consequently the synthesized guidance command is free from abrupt-jumping phenomenon. Numerical simulations and performance comparison fully demonstrates the effectiveness and superiority of the proposed guidance law.

INDEX TERMS Barrier Lyapunov function, FOV constraint, impact angle control, dynamic surface control.

I. INTRODUCTION

Imposing desired terminal engagement geometries is increasingly required by advanced guidance laws in the one or a combination of the following applications: exploiting the weak points of the target, increasing the warhead effectiveness, avoiding directional defense mechanisms, adjusting the time of arrival, reducing the collateral damage, etc [1]. The impact angle control guidance law that is able to shape the missile trajectory without decreasing the miss distance value has become an important research focus.

There are quite a number of studies on impact angle control in the literature. Based on the proportional navigation (PN), shaping the trajectory and consequently the impact geometry were achieved in an early work by adding a time-varying bias to PN commands [2]. In [3]–[5], the two-phase guidance schemes with impact angle constraint were proposed successively. The two-phase guidance scheme suggested in [3] used a lower navigation gain to generate the orientation guidance command in the first stage, followed by a conventional second stage that used a higher navigation to impose the desired impact angle. In [4], this guidance scheme was further extended to the case of moving targets. Combining biased PN and pure PN, the two-phase guidance law developed in [5] involved continuous integration of a constant bias for the initial phase and its subsequent removal after the integral reaches a certain value calculated from initial engagement conditions and desired impact angle. Without using any switching logic or bias term, a novel nonswitching guidance law that had a similar structure to the conventional PN was recently proposed in [6], whose guidance command was expressed as a function of line-of-sight (LOS) angle and its angular rate to achieve desired impact angles against a stationary target. Apart from PN-based guidance law, the optimal control theory was also extensively applied to address the impact angle control problem. Most of existing optimal impact angle control guidance laws are similar in their structures, but change the cost function to achieve a specific guidance purpose, such as minimizing overall control effort (quadratic cost function) [7], alleviating sensitivity to initial heading error (polynomial/sinusoidal weighting function [8], [9]), shaping the trajectory and acceleration profiles

The associate editor coordinating the review of this manuscript and approving it for publication was Bidyadhar Subudhi.

This work is licensed under a Creative Commons Attribution-NonCommercial-NoDerivatives 4.0 License.
For more information, see https://creativecommons.org/licenses/by-nc-nd/4.0/

(Gaussian weighting function) [10], enhancing robustness to external disturbances or uncertainties (power weighing function) [11], and distributing acceleration demand against the loss of aerodynamic maneuverability (exponential weighting function) [12]. Although such a great number of optimal impact angle control guidance laws have been proposed, how to understand and analyze the nature of these guidance laws to facilitate evaluating their reliability and predicting their performance in practical applications is still unclear. Until recently, Lee and Seo focused on this problem and corrected previous inaccurate interpretations to reunderstand the characteristics of optimal guidance laws, thereby providing a new guideline for selecting appropriate gain that reflects the physical meaning [13].

Independent of various guidance objectives, all missiles are subject to physical constraints. Imposing a terminal impact angle always makes the missile trajectory highly curved and is easily prone to losing the target from the maximum seeker's field-of-view (FOV), even mission failure. Although handling the FOV constraint is of great important and urgent practical need, it is rarely considered in the existing study of impact angle control.

The studies focusing on the FOV constraint mainly have their foundation within the framework of the optimal control theory. The first investigation in this direction was completed by Xin *et al.* [14], wherein the $\theta - D$ nonlinear control approach was used to address the FOV constraint and a closed-form optimal guidance law was designed. In [15], Park *et al.* proposed an optimal guidance law based on optimal control theory with state inequality constraint, and further improved it in [16] to redistribute the control energy along the flight trajectory, thereby maximizing the warhead effect. Assuming the optimal guidance law as a polynomial function of time-to-go, Lee *et al.* proposed to determine the coefficients of the guidance command based on the worst case to guarantee the FOV constraint not to be violated in [17]. To address the FOV constraint, a varying coefficient of weighted optimal control guidance law was recently proposed in [18], whose changeable weighting coefficients provided an additional degree of freedom to shape the missile trajectory while maintaining the lock-on condition. Also, there are other forms of impact angle guidance laws developed to address the FOV constraint, although they do not claim optimality. A good example is the PN guidance law that is enhanced by switching navigation gain/bias term logic. Generally, the early studies in this direction selected the navigation gain as $N = 1$ to constrain the maximum look angle at the first phase and $N \geq 2$ to achieve the desired impact angle at the second phase [19], [20]. To be more precisely, the values of navigation gains at midcourse and terminal stages were calculated by a numerical algorithm proposed by Tekin and Erer in [1]. Moreover, Ratnoo discussed the choice of navigation gains in [21] to achieve all possible impact angles without violating the FOV constraint. As for the biased PN guidance law, its pioneering examples were those of Park *et al.*, wherein a bias-shaping addition were added to the classical PN guidance command to intercept stationary [22] and moving [23] targets at a desired impact angle under the FOV constraint.

A novel impact angle control guidance law considering the FOV constraint is proposed in this article. The FOV constraint, actually imposed on the body-LOS (BLOS) angle, is equally transformed to a time-varying asymmetric limitation on the component of missile-target relative velocity perpendicular to the missile-target LOS. Based on the dynamic surface control and time-varying asymmetric Barrier Lyapunov Function (BLF), this relative velocity component can be forced to approach zero to meet the homing requirement while being prevented from overstepping its time-varying asymmetric limitation to satisfy the FOV constraint. Compared to previous studies, the linearization of the engagement equations and the estimation of time-to-go, which are always required by the optimal impact angle control guidance law, is no longer need to be implemented. On the contrary, a nonlinear engagement dynamics that considers the variation of the missile velocity, the evading maneuver of the target, and the effect of the gravity is modeled and used during the process of guidance design. Moreover, different from modified PN guidance laws, the proposed guidance law do not involve any switching logic and consequently generate smooth guidance command, thus avoiding the abrupt-jumping phenomenon.

The remainder of this article is organized as follows. Section II presents this guidance problem and introduces some preliminaries for the base of subsequent guidance design. The time-varying asymmetric BLF-based impact angle control guidance law is presented in Section III in detail, and also the guidance performance analysis is given. To fully testify the performance of the proposed guidance law, extensive numerical simulations and performance comparison for simplified and realistic missile models against both stationary and moving target are carried out in Section IV. The conclusion in Section V ends this article.

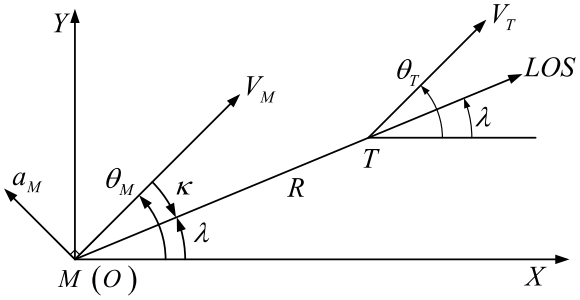

FIGURE 1. Two-dimensional homing scenario.

II. PROBLEM FORMULATION AND PRELIMINARIES

A. PROBLEM FORMULATION

Consider a two-dimensional homing scenario shown in Fig. 1, where a roll stabilized axisymmetric missile and a stationary/moving ground target are marked as M and T in the

inertial coordinate system OXY, respectively. For the sake of guidance law design, the missile and target are assumed to be point masses, and dynamics of autopilot and actuator are fast enough to be neglected. The corresponding engagement dynamics is given by

$$\dot{R} = V_T \cos(\theta_T - \lambda) - V_M \cos(\theta_M - \lambda) \tag{1}$$
$$R\dot{\lambda} = V_T \sin(\theta_T - \lambda) - V_M \sin(\theta_M - \lambda) \tag{2}$$
$$\dot{\theta}_M = \frac{a_M}{V_M} \tag{3}$$
$$\dot{\theta}_T = 0 \tag{4}$$

where R denotes the missile-target relative distance, and λ denotes the missile-target LOS angle. V_M and V_T denote the missile velocity and target velocity, θ_M and θ_T denote the flight-path angle of the missile and target, respectively. κ denotes the missile leading angle, and a_M denotes the missile lateral acceleration normal to its velocity. All angles are defined as positive in the counterclockwise direction.

To maintain the lock-on condition during the whole homing phase, the BLOS angle, which is defined as the angle between the missile body axis and the missile-target LOS, should always be confined within the FOV of the missile seeker. Generally, the optical axis of the missile seeker is aligned with the missile body axis, and thus the BLOS angle can be regarded as the sum of the missile leading angle κ and the angle of attack α in the longitudinal plane. Under the assumption that the missile's angle of attack is small enough (this is a commonly-used assumption in previous studies), the BLOS angle can be further approximated by the leading angle. Thus, the FOV constraint is equivalently transformed to $|\kappa| < \kappa_{\max}$, where $\kappa_{\max}$ is a positive constant determined by the FOV constraint.

Because the lead angle cannot be measured in practice, it is difficult to directly limit the lead angle within a certain range. Alternatively, this constraint on the leading angle can be achieved by restricting the missile-target relative velocity to the neighborhood of the LOS. Therefore, define the components of the missile-target relative velocity along and perpendicular to the LOS as

$$V_R = \dot{R} \tag{5}$$
$$V_\lambda = R\dot{\lambda} \tag{6}$$

Differentiating (6) and substituting (1)–(5) yields

$$\dot{V}_\lambda = -\frac{V_R V_\lambda}{R} - a_M \cos(\theta_M - \lambda) + d \tag{7}$$
$$d = \dot{V}_T \sin(\theta_T - \lambda) - \dot{V}_M \sin(\theta_M - \lambda) \tag{8}$$

where d denotes the lumped disturbance caused by unknown target maneuver and the missile velocity change.

Note that the lumped disturbance d cannot be measured precisely in practice. However, the maneuver capacities of the missile and target are both bounded due to the physical limit, it is thus reasonable to make the following assumption.

Assumption 1: During the homing phase, the disturbance d is always bounded, namely $|d| \le D$, where D is a positive constant.

Define two new variables as

$$k_{b_1} = V_T \sin(\theta_T - \lambda) - V_M \sin\kappa_{\max} \tag{9}$$
$$k_{b_2} = V_T \sin(\theta_T - \lambda) + V_M \sin\kappa_{\max} \tag{10}$$

Generally, the missile has a great speed advantage over the target, it follows that $V_T < V_M \sin\kappa_{\max}$. Thus, we have

$$\begin{aligned} k_{b_1} &= V_T \sin(\theta_T - \lambda) - V_M \sin\kappa_{max} \\ &\le V_T - V_M \sin\kappa_{\max} < 0 \end{aligned} \tag{11}$$
$$\begin{aligned} k_{b_2} &= V_T \sin(\theta_T - \lambda) + V_M \sin\kappa_{max} \\ &\ge -V_T + V_M \sin\kappa_{\max} > 0 \end{aligned} \tag{12}$$

Without loss of any generality, the following assumption is made.

Assumption 2: The lock-on condition at the begin of homing phase is satisfied, namely $|\kappa(t_0)| < \kappa_{\max}$.

Then the following lemma is introduced to handle the FOV constraint.

Lemma 1: Under Assumption 2, the FOV constraint will never be violated if the inequality $k_{b_1} < V_\lambda < k_{b_2}$ always holds during the homing phase.

Proof: Supposing that Assumption 2 is satisfied, the inequality $k_{b_1} < V_\lambda < k_{b_2}$ can be rewritten by combining (2), (6), (9), and (10) as

$$\begin{aligned} &V_T \sin(\theta_T - \lambda) - V_M \sin\kappa_{\max} < V_T \sin(\theta_T - \lambda) \\ &-V_M \sin(\theta_M - \lambda) < V_T \sin(\theta_T - \lambda) + V_M \sin\kappa_{\max} \end{aligned} \tag{13}$$

namely

$$-\sin\kappa_{\max} < \sin\kappa < \sin\kappa_{\max} \tag{14}$$

that is $|\kappa| < \kappa_{\max}$, thus meeting the FOV constraint. ■

Given that the target velocity can hardly be measured accurately in practice, the variables k_{b_1}, k_{b_2}, according to (2), is rewritten as

$$k_{b_1} = R\dot{\lambda} + V_M \sin(\theta_M - \lambda) - V_M \sin\kappa_{\max} \tag{15}$$
$$k_{b_2} = R\dot{\lambda} + V_M \sin(\theta_M - \lambda) + V_M \sin\kappa_{\max} \tag{16}$$

Remark 1: By Lemma 1, the FOV constraint on the leading angle κ is finally transformed to a time-varying asymmetric limitation on the component of the missile-target relative velocity perpendicular to the LOS V_λ. Besides, according to the parallel approach method, a sufficient condition of a precise attack is to point the missile velocity to the target. That is, V_λ should be forced to approach zero for homing requirement. Thus, both the homing requirement and the FOV constraint boil down to one control variable V_λ, which greatly simplifies the guidance law design.

Just as [25], [26], the impact angle in this study is defined as the LOS angle at the impact time λ_d. Then the final nonlinear guidance model is derived based on (6)–(7) as

$$\begin{cases} \dot{\lambda} = \dfrac{V_\lambda}{R} \\ \dot{V}_\lambda = -\dfrac{V_R V_\lambda}{R} - a_M \cos(\theta_M - \lambda) + d \end{cases} \tag{17}$$

For this guidance model, the control objective is to design the guidance law a_M to guarantee that $V_\lambda \to 0$ for the homing requirement, $\lambda \to \lambda_d$ for the impact angle constraint, and $k_{b_1} < V_\lambda < k_{b_2}$ always holds for the FOV constraint.

B. PRELIMINARY

To handle the time-varying asymmetric limitation on V_λ, according to [26], an asymmetric smooth saturation function is introduced as

$$\mathrm{Tanh}(x, k_1, k_2) = \frac{\mathrm{e}^{x} - \mathrm{e}^{-x}}{-\dfrac{\mathrm{e}^{x}}{k_1} + \dfrac{\mathrm{e}^{-x}}{k_2}} \tag{18}$$

where $x \in \mathbb{R}$, $k_1 < 0$ and $k_2 > 0$ are two variables. The graph of $\mathrm{Tanh}(x, k_1, k_2)$ with constant k_1 and k_2 is shown in Fig. 2.

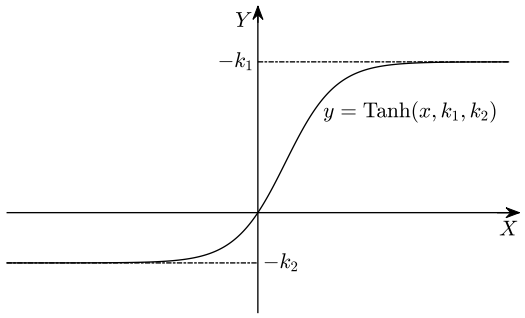

FIGURE 2. The graph of $\mathrm{Tanh}(x, k_1, k_2)$.

The function $\mathrm{Tanh}(x, k_1, k_2)$ has the following two properties, and their proof can be found in [26].

Property 1: The inequality $-k_2 < \mathrm{Tanh}(x, k_1, k_2) < -k_1$ for $\forall x \in \mathbb{R}$ holds.

Property 2: The function $x\,\mathrm{Tanh}(x, k_1, k_2)$ is a positive definite function.

Then several important lemmas are presented for the sake of subsequent guidance law design.

Lemma 2: For any positive constants k_{a_1} and k_{b_1}, let $\mathcal{Z}_1 := \{z_1 \in \mathbb{R} : -k_{a_1} < z_1 < k_{b_1}\} \subset \mathbb{R}$ and $\mathcal{N} := \mathbb{R}^l \times \mathcal{Z}_1 \subset \mathbb{R}^{l+1}$ be open sets. Consider the system

$$\dot{\eta} = h(t, \eta) \tag{19}$$

where the system state η is split into free states ω and the constrained state z_1, namely $\eta := [\omega, z_1]^{\mathrm{T}} \in \mathcal{N}$ and $h := \mathbb{R}_+ \times \mathcal{N} \to \mathbb{R}^{l+1}$ is piecewise continuous in t and locally Lipschitz in z, uniformly in t, on $\mathbb{R}_+ \times \mathcal{N}$. Suppose that there exist functions $U : \mathbb{R}^l \to \mathbb{R}_+$ and $V_1 : \mathcal{Z}_1 \to \mathbb{R}_+$, continuously differentiable and positive definite in their respective domains, such that

$$V_1(z_1) \to \infty \quad \text{as } z_1 \to -k_{a_1} \text{ or } z_1 \to k_{b_1} \tag{20}$$

$$\gamma_1(\|\omega\|) \le U(\omega) \le \gamma_2(\|\omega\|) \tag{21}$$

where γ_1 and γ_2 are class K_∞ functions. Let $V(\eta) := V_1(z_1) + U(\omega)$, and $z_1(0)$ belongs to the set $z_1 \in (-k_{a_1}, k_{b_1})$. If the inequality holds:

$$\dot{V} = \frac{\partial V}{\partial \eta} h \le 0 \tag{22}$$

then $z_1(t)$ remains in the open set $z_1 \in (-k_{a_1}, k_{b_1})$ for $\forall t \in [0, \infty)$. The proof can be found in [27].

Remark 2: In Lemma 2, the function V_1 that satisfies condition (20) is called BLF, which prevents the constrained system state from reaching its boundary. According to the boundary character, a BLF could be symmetric or asymmetric as shown in Fig. 3.

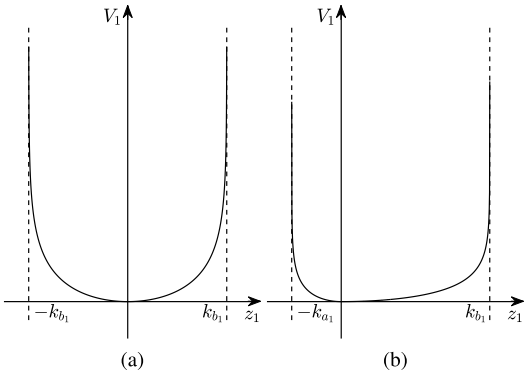

FIGURE 3. Symmetric (left) and asymmetric (right) BLF.

Lemma 3: For any positive constant k, if s in the interval of $|s| < k$, s will satisfy the following inequality

$$\frac{s^2}{k^2} \le \log \frac{k^2}{k^2 - s^2} \le \frac{s^2}{k^2 - s^2} \tag{23}$$

where the equal sign holds if and only if $s = 0$. The proof is given in Appendix.

III. TABLF-BASED GUIDANCE LAW DESIGN

A. DYNAMIC SURFACE CONTROLLER DESIGN

Noting that the guidance model (17) has a strict feedback structure, the dynamic surface control technique is then employed to design the guidance law.

Step 1: Considering the impact angle constraint, define the sliding surface s_1 for the system state λ as

$$s_1 = \lambda - \lambda_d \tag{24}$$

Define a quadratic Lyapunov function candidate for the sliding surface s_1 as

$$V_1 = \frac{1}{2} s_1^2 \tag{25}$$

Differentiating V_1 yields

$$\dot{V}_1 = s_1 \dot{s}_1 = s_1 \dot{\lambda} = s_1 \frac{V_\lambda}{R} \tag{26}$$

To make $\dot{V}_1$ negative definite, it is required that $s_1 \dot{s}_1 < 0$. Regarding V_λ as a virtual control input and considering the time-varying asymmetric limitation $k_{b_1} < V_\lambda < k_{b_2}$,

the desired feedback control is designed based on the asymmetric smooth saturation function as

$$V_{\lambda_d} = -\operatorname{Tanh}(k_1 s_1, k_{a_1}, k_{a_2}) \tag{27}$$

where design parameter $k_1 > 0$. k_{a_1} and k_{a_2} denote the maximum admissible boundaries of V_{λ_d} and satisfies

$$k_{a_1} = k_{b_1} + \epsilon < 0 \tag{28}$$
$$k_{a_2} = k_{b_2} - \epsilon > 0 \tag{29}$$

where ϵ is a small positive constant.

Remark 3: The introduction of $\operatorname{Tanh}(k_1 s_1, k_{a_1}, k_{a_2})$ ensures that the time-varying asymmetric limitation $k_{b_1} < V_\lambda < k_{b_2}$ always holds according to Property 1, and $s_1 \dot{s}_1 < 0$ is also satisfied on the basis of Property 2.

Remark 4: The saturation characteristic of $\operatorname{Tanh}(k_1 s_1, k_{a_1}, k_{a_2})$ allows the missile-target relative velocity to approach the LOS at the maximum allowable turning rate when the system state λ is far from the sliding surface s_1, thus making sliding surface s_1 converge to zero as soon as possible. Moreover, by choosing a larger design parameter k_1, the time for maintaining V_λ at the maximum allowable boundary can be further extended to make the best use of the available FOV of the seeker, which makes the missile trajectory as curved as possible, thereby achieving a larger impact angle.

To avoid the problem of ''explosion of the complexity'', let V_{λ_d} pass through the following first-order filter with time constant τ_1

$$\tau_1 \dot{V}_{\lambda_c} + V_{\lambda_c} = V_{\lambda_d} \tag{30}$$

Define the tracking error of the first-order filter (30) as

$$\mu_1 = V_{\lambda_c} - V_{\lambda_d} \tag{31}$$

Step 2: To track the virtual control input V_{λ_c}, define the sliding surface s_2 for the system state V_λ as

$$s_2 = V_\lambda - V_{\lambda_c} \tag{32}$$

Combining (26), (27), (31) and (32), the derivative of quadratic Lyapunov function V_1 (25) can be rewritten as

$$\begin{aligned}\dot{V}_1 &= s_1 \frac{V_\lambda}{R} \\ &= s_1 \frac{s_2 + \mu_1 + V_{\lambda_d}}{R} \\ &\le \frac{s_1 s_2}{R} + \frac{1}{2} s_1^2 + \frac{\mu_1^2}{2R_f} - \frac{s_1}{R} \operatorname{Tanh}(k_1 s_1, k_{a_1}, k_{a_2})\end{aligned} \tag{33}$$

where R_f denote the final relative distance at the impact time.

Differentiating s_2 yields

$$\dot{s}_2 = -\frac{V_R V_\lambda}{R} - a_M \cos(\theta_M - \lambda) + d - \dot{V}_{\lambda_c} \tag{34}$$

Considering time-varying asymmetric limitation on V_λ, according to [28], define a time-varying asymmetric BLF (TABLF) for the sliding surface s_2 as

$$V_2 = \frac{1-p}{2} \log \frac{k_{c_1}^2}{k_{c_1}^2 - s_2^2} + \frac{p}{2} \log \frac{k_{c_2}^2}{k_{c_2}^2 - s_2^2} + \frac{1}{2\gamma} \tilde{D}^2 \tag{35}$$

where the time-varying upper and lower boundaries with respect to s_2 is defined as

$$k_{c_1} = V_{\lambda_c} - k_{b_1} > 0 \tag{36}$$
$$k_{c_2} = k_{b_2} - V_{\lambda_c} > 0 \tag{37}$$

The selecting function $p(s_2)$ is defined as

$$p(s_2) = \begin{cases} 1, & 0 < s_2 < k_{c_2} \\ 0, & -k_{c_1} < s_2 \le 0 \end{cases} \tag{38}$$

and the adaptive estimation error $\tilde{D}$ is defined as

$$\tilde{D} = D - \hat{D} \tag{39}$$

where $\hat{D}$ is the estimation of D, the unknown upper boundary of the lumped disturbance d. The design parameter $\gamma > 0$.

Note that for $\forall s_2 \in (-k_{c_1}, k_{c_2})$, $V_2 \ge 0$, and only if $s_2 = 0$, $V_2 = 0$. Therefore, V_2 is positive definite. Meanwhile, $\dot{V}_2$ is continuous within each of the two intervals $s_2 \in (-k_{c_1}, 0)$ and $s_2 \in (0, k_{c_2})$, respectively. Also, $\lim_{s_2 \to 0^+} \mathrm{d}V_2/\mathrm{d}s_2 = \lim_{s_2 \to 0^-} \mathrm{d}V_2/\mathrm{d}s_2$. It implies that V_2 is continuously differentiable. Thus, V_2 is a valid Lyapunov Function candidate.

Differentiating V_2 yields, (40), as shown at the bottom of the page.

Let

$$\Theta = \frac{1-p}{k_{c_1}^2 - s_2^2} + \frac{p}{k_{c_2}^2 - s_2^2} > 0 \tag{41}$$

and substituting (34) into the above equation yields

$$\begin{aligned}\dot{V}_2 = s_2 \Theta \Bigg[&-\frac{V_R V_\lambda}{R} - a_M \cos(\theta_M - \lambda) + d - \dot{V}_{\lambda_c} \\ &- \Big(1-p\Big)\frac{\dot{k}_{c_1}}{k_{c_1}} s_2 - p \frac{\dot{k}_{c_2}}{k_{c_2}} s_2 \Bigg] + \frac{1}{\gamma} \tilde{D} \dot{\tilde{D}}\end{aligned} \tag{42}$$

$$\begin{aligned}\dot{V}_2 &= s_2 \frac{1-p}{k_{c_1}^2 - s_2^2} \left(\dot{s}_2 - \frac{\dot{k}_{c_1}}{k_{c_1}} s_2 \right) + s_2 \frac{p}{k_{c_2}^2 - s_2^2} \left(\dot{s}_2 - \frac{\dot{k}_{c_2}}{k_{c_2}} s_2 \right) + \frac{1}{\gamma} \tilde{D} \dot{\tilde{D}} \\ &= s_2 \left(\frac{1-p}{k_{c_1}^2 - s_2^2} + \frac{p}{k_{c_2}^2 - s_2^2} \right) \left[\dot{s}_2 - \Big(1-p\Big)\frac{\dot{k}_{c_1}}{k_{c_1}} s_2 - p \frac{\dot{k}_{c_2}}{k_{c_2}} s_2 \right] + \frac{1}{\gamma} \tilde{D} \dot{\tilde{D}}\end{aligned} \tag{40}$$

Then design the real control input command a_{M_c} as

$$a_{M_c} = \frac{-1}{\cos(\theta_M - \lambda)}\left[\frac{V_R V_\lambda}{R} + \dot{V}_{\lambda_c} - \left(k_2 + \bar{k}_2\right)s_2 - \hat{D}\,\mathrm{sgn}(s_2)\right] \tag{43}$$

where the design parameters $k_2 > 0, l_2 > 0$, and time-varying parameter $\bar{k}_2$ is

$$\bar{k}_2 = \sqrt{\left(1-p\right)\left(\frac{\dot{k}_{c_1}}{k_{c_1}}\right)^2 + p\left(\frac{\dot{k}_{c_2}}{k_{c_2}}\right)^2 + \beta} \tag{44}$$

where the design parameter $\beta > 0$.

The adaptive law is designed as

$$\dot{\hat{D}} = \gamma\Theta\,|s_2| \tag{45}$$

Substituting (43) into (42) yields

$$\dot{V}_2 = s_2\Theta\left\{\left[k_2 + \bar{k}_2 + \left(1-p\right)\frac{\dot{k}_{c_1}}{k_{c_1}} + p\frac{\dot{k}_{c_2}}{k_{c_2}}\right]s_2 - \hat{D}\,\mathrm{sgn}(s_2) + d\right\} + \frac{1}{\gamma}\tilde{D}\dot{\tilde{D}} \tag{46}$$

Let

$$K_2 = \bar{k}_2 + \left(1-p\right)\frac{\dot{k}_{c_1}}{k_{c_1}}s_2 + p\frac{\dot{k}_{c_2}}{k_{c_2}} \tag{47}$$

because $\beta > 0$, $K_2 > 0$ always holds.

Substituting K_2 into (46), $\dot{V}_2$ is further rewritten as

$$\begin{aligned}\dot{V}_2 &= s_2\Theta\left[-\left(k_2 + K_2\right)s_2 - \hat{D}\,\mathrm{sgn}(s_2) + d\right] + \frac{1}{\gamma}\tilde{D}\dot{\tilde{D}} \\ &= -\Theta\left(k_2 + K_2\right)s_2^2 - \Theta\left(D|s_2| - ds_2\right) + \Theta\tilde{D}|s_2| + \frac{1}{\gamma}\tilde{D}\dot{\tilde{D}} \\ &\le -\Theta\left(k_2 + K_2\right)s_2^2 - \Theta\left(D - |d|\right)|s_2| + \tilde{D}\left(\Theta|s_2| + \frac{1}{\gamma}\dot{\tilde{D}}\right) \\ &\le -\Theta\left(k_2 + K_2\right)s_2^2\end{aligned} \tag{48}$$

Note that the unknown derivatives of the time-varying boundaries k_{c_1}, k_{c_2} are included in the control input command a_{M_c}. Therefore, let k_{c_1}, k_{c_2} pass through the following first-order filter

$$\tau_{i+1}\dot{k}_{d_i} + k_{d_i} = k_{c_i}, \qquad i = 1, 2 \tag{49}$$

where τ_2, τ_3 are the time constants of the first-order filters, and the corresponding tracking error are

$$\mu_{i+1} = k_{d_i} - k_{c_i}, \qquad i = 1, 2 \tag{50}$$

Hereto, the proposed TABLF-based impact angle control guidance law can be summarized as

$$\begin{cases} s_1 = \lambda - \lambda_d \\ k_{b_1} = R\dot{\lambda} + V_M\sin(\theta_M - \lambda) - V_M\sin\kappa_{max} \\ k_{b_2} = R\dot{\lambda} + V_M\sin(\theta_M - \lambda) + V_M\sin\kappa_{max} \\ k_{a_1} = k_{b_1} + \epsilon \\ k_{a_2} = k_{b_2} - \epsilon \\ V_{\lambda_d} = -\,\mathrm{Tanh}(k_1 s_1, k_{a_1}, k_{a_2}) \\ \dot{V}_{\lambda_c} = -\dfrac{V_{\lambda_c}}{\tau_1} + \dfrac{V_{\lambda_d}}{\tau_1} \\ s_2 = V_\lambda - V_{\lambda_c} \\ k_{c_1} = V_{\lambda_c} - k_{b_1} \\ k_{c_2} = k_{b_2} - V_{\lambda_c} \\ \dot{k}_{d_i} = -\dfrac{k_{d_i}}{\tau_{i+1}} + \dfrac{k_{c_i}}{\tau_{i+1}}, \qquad i = 1, 2 \\ p = \begin{cases} 1, & 0 < s_2 < k_{c_2} \\ 0, & -k_{c_1} < s_2 \le 0 \end{cases} \\ \bar{k}_2 = \sqrt{\left(1-p\right)\left(\dfrac{\dot{k}_{d_1}}{k_{c_1}}\right)^2 + p\left(\dfrac{\dot{k}_{d_2}}{k_{c_2}}\right)^2 + \beta} \\ \Theta = \dfrac{1-p}{k_{c_1}^2 - s_2^2} + \dfrac{p}{k_{c_2}^2 - s_2^2} \\ \dot{\hat{D}} = \gamma\Theta|s_2| \\ a_{M_c} = \dfrac{-1}{\cos(\theta_M - \lambda)}\left[\dfrac{V_R V_\lambda}{R} + \dot{V}_{\lambda_c} - \left(k_2 + \bar{k}_2\right)s_2 - \hat{D}\,\mathrm{sgn}(s_2)\right] \end{cases} \tag{51}$$

B. THE GUIDANCE PERFORMANCE ANALYSIS

The tracking error of the first-order filter (30) satisfies

$$\dot{\mu}_1 = -\frac{\mu_1}{\tau_1} - \dot{V}_{\lambda_d} \tag{52}$$

The tracking error of the first-order filter (49) satisfies

$$\dot{\mu}_{i+1} = -\frac{\mu_{i+1}}{\tau_{i+1}} - \dot{k}_{c_i}, \qquad i = 1, 2 \tag{53}$$

Generally, the derivative of virtual control input is continuous and bounded [29]. Let

$$\Lambda = \max\left(\sup_{t\in[t_0,t_f]}\left|\dot{V}_{\lambda_d}(t)\right|, \sup_{t\in[t_0,t_f]}\left|\dot{k}_{c_1}(t)\right|, \sup_{t\in[t_0,t_f]}\left|\dot{k}_{c_2}(t)\right|\right) \tag{54}$$

then the tracking error u_i of the first-order filters (30) and (49) further satisfy

$$\mu_i\dot{\mu}_i \le -\frac{\mu_i^2}{\tau_i} + |\mu_i|\Lambda \le -\frac{\mu_i^2}{\tau_i} + \frac{\mu_i^2}{2} + \frac{\Lambda^2}{2}, \quad i = 1, 2, 3 \tag{55}$$

Define a quadratic Lyapunov function candidate for the tracking error μ_i as

$$V_3 = \frac{1}{2}\sum_{i=1}^{3}\mu_i^2 \tag{56}$$

According to (55), the derivative of V_3 satisfies

$$\dot{V}_3 = \sum_{i=1}^{3} \mu_i \dot{\mu}_i \le -\sum_{i=1}^{3} \frac{\mu_i^2}{\tau_i} + \sum_{i=1}^{3} \frac{\mu_i^2}{2} + \frac{3\Lambda^2}{2} \tag{57}$$

Define a Lyapunov function for the closed-loop system as

$$V = V_1 + V_2 + V_3 \tag{58}$$

Combining (33), (48) and (57), the derivative of the closed-loop Lyapunov function satisfies

$$\begin{aligned} \dot{V} \le\ & s_1^2 + \frac{s_2^2}{2R_{f_1}} - \Theta\left(k_2 + K_2\right)s_2^2 \\ & - \frac{s_1}{R}\,\mathrm{Tanh}\left(k_1 s_1, k_{a_1}, k_{a_2}\right) - \left(\frac{1}{\tau_1} - \frac{1}{2R_f} - \frac{1}{2}\right)\mu_1^2 \\ & - \left(\frac{1}{\tau_2} - \frac{1}{2}\right)\mu_2^2 - \left(\frac{1}{\tau_3} - \frac{1}{2}\right)\mu_3^2 + \frac{3\Lambda^2}{2} \end{aligned} \tag{59}$$

According to Property 2, $s_1\,\mathrm{Tanh}(k_1 s_1, k_{a_1}, k_{a_2}) \ge 0$, and based on Lemma 3, the above equation is rewritten as

$$\begin{aligned} \dot{V} \le\ & s_1^2 + \frac{s_2^2}{2R_{f_1}} - \left(\frac{1}{\tau_1} - \frac{1}{2R_f} - \frac{1}{2}\right)\mu_1^2 \\ & - 2\left(k_2 + K_2\right)\left(\frac{1-p}{2}\log\frac{k_{c_1}^2}{k_{c_1}^2 - s_2^2} + \frac{p}{2}\log\frac{k_{c_2}^2}{k_{c_2}^2 - s_2^2}\right) \\ & - \left(\frac{1}{\tau_2} - \frac{1}{2}\right)\mu_2^2 - \left(\frac{1}{\tau_3} - \frac{1}{2}\right)\mu_3^2 + \frac{3\Lambda^2}{2} \end{aligned} \tag{60}$$

Choose design parameter k_2 and the time constant τ_i to satisfy the following inequalities

$$\begin{cases} K \le 2\left(k_2 + K_2\right) \\ \dfrac{K}{2} \le \dfrac{1}{\tau_1} - \dfrac{1}{2R_f} - \dfrac{1}{2} \\ \dfrac{K}{2} \le \dfrac{1}{\tau_2} - \dfrac{1}{2} \\ \dfrac{K}{2} \le \dfrac{1}{\tau_3} - \dfrac{1}{2} \end{cases} \tag{61}$$

where $K > 0$ is a constant.

Then the derivative of the closed-loop Lyapunov function (60) is further revised as

$$\begin{aligned} \dot{V} \le\ & -\frac{K}{2}s_1^2 - \frac{K}{2}\sum_{i=1}^{3}\mu_i^2 \\ & - K\left(\frac{1-p}{2}\log\frac{k_{c_1}^2}{k_{c_1}^2 - s_2^2} + \frac{p}{2}\log\frac{k_{c_2}^2}{k_{c_2}^2 - s_2^2} + \frac{1}{2\gamma}\tilde{D}^2\right) \\ & + \left(1 + \frac{K}{2}\right)s_1^2 + \frac{s_2^2}{2R_f} + \frac{K}{2\gamma}\tilde{D}^2 + \frac{3\Lambda^2}{2} \end{aligned} \tag{62}$$

Noting that the sliding surface s_1 is defined as the deviation between the LOS angle λ and the desired impact angle λ_d, this deviation would not be greater than 180° in practice, namely $|s_1| \le \pi$, thus

$$\frac{1+K}{2}s_1^2 \le \frac{1+K}{2}\pi^2 \tag{63}$$

Let $\Gamma = \max\left(k_{c_1}(t), k_{c_2}(t)\right)$, according to the definition of the TABLF V_2, for $\forall s_2 \in \left(-k_{c_1}, k_{c_2}\right)$ (35), we have

$$\frac{s_2^2}{2R_f} \le \frac{\Gamma^2}{2R_f} \tag{64}$$

According to the definition of the adaptive estimation error $\tilde{D}$ (39) and the adaptive law (45), it follows that

$$\dot{\tilde{D}} = -\gamma\Theta|s_2| \le 0 \tag{65}$$

which implies that adaptive estimation error function $\tilde{D}(t)$ is a non-increasing function. Assuming that $\hat{D}(t_0)$, the initial estimation of the unknown upper boundary D is zero, then the adaptive estimation error $\tilde{D}$ satisfies

$$\begin{aligned} \left|\tilde{D}(t)\right| &\le \max\left(\tilde{D}(t_0), \tilde{D}(t_f)\right) \\ &= \max\left(D, D - \hat{D}(t_f)\right) = \Pi \end{aligned} \tag{66}$$

Let

$$\left(1 + \frac{K}{2}\right)\pi^2 + \frac{\Gamma^2}{2R_f} + \frac{K}{2\gamma}\Pi^2 + \frac{3\Lambda^2}{2} = c \tag{67}$$

then according to Lemma 3, equation (62) is finally rewritten as

$$\dot{V} \le -KV + c \tag{68}$$

Hereto, the guidance performance of the proposed TABLF-based impact angle control guidance law can be guaranteed based on the following Theorem.

Theorem 1: Supposing that Assumptions 1–2 are satisfied, the guidance model (17) under the proposed TABLF-based impact angle control guidance law (51) has the following properties:

1) Both sliding surfaces s_1, s_2 are uniform ultimately bounded and converge into the compact sets

$$|s_1(t)| \le \sqrt{2\left[\rho + V(0)\right]}|s_2(t)| \le \sqrt{\frac{2}{\Theta'}\left[\rho + V(0)\right]} \tag{69}$$

where $\rho = \dfrac{c}{K}$, $\Theta' = \dfrac{1-p}{k_{c_1}^2} + \dfrac{p}{k_{c_2}^2}$.

2) For $\forall t \ge 0$, the component of missile-target relative velocity perpendicular to the LOS V_λ always satisfies the time-varying asymmetric limitation $k_{b_1}(t) < V_\lambda(t) < k_{b_2}(t)$ and eventually converges to zero.
3) All closed-loop signals are bounded.

Proof:

1) Let $\rho = \dfrac{c}{K}$, and direct integrating of the differential inequality (68) yields

$$0 \le V(t) \le \rho + \left[V(0) - \rho\right]\mathrm{e}^{-Kt} \le \rho + V(0) \tag{70}$$

Let $\Theta' = \dfrac{1-p}{k_{c_1}^2} + \dfrac{p}{k_{c_2}^2}$, and according to Lemma 3, it follows that

$$\frac{\Theta'}{2}s_2^2 \le \frac{1-p}{2}\log\frac{k_{c_1}^2}{k_{c_1}^2 - s_2^2} + \frac{p}{2}\log\frac{k_{c_2}^2}{k_{c_2}^2 - s_2^2} \tag{71}$$

Combining (25), (35), (56), (58) and (71) yields

$$\frac{1}{2}s_1^2 + \frac{\Theta'}{2}s_2^2 + \frac{1}{2}\mu^2 \leq V_1 + V_2 + V_3 = V \quad (72)$$

then combining (70) and (72) yields

$$|s_1(t)| \leq \sqrt{2\left[\rho + V(0)\right]}|s_2(t)| \leq \sqrt{\frac{2}{\Theta'}\left[\rho + V(0)\right]}$$

2) It is known from (70) that the closed-loop Lyapunov function $V(t)$ is bounded. Assuming that there exists some $t = T$ such that $V_\lambda(T) = k_{b_1}$ or $V_\lambda(T) = k_{b_2}$, the sliding surface s_2 tends to approach its boundary, namely $s_2 \to -k_{c_1}$ or $s_2 \to k_{c_2}$. According to (35), when s_2 approach its boundary, $V(T)$ becomes unbounded, which obviously contradicts the boundedness of $V(t)$. Therefore, the time-varying asymmetric limitation $k_{b_1}(t) < V_\lambda(t) < k_{b_2}(t)$ always holds for $\forall t \geq 0$.
From (27) and (43), it is known that sliding surfaces are both designed to converge to zeros. When $s_1 \to 0$, $V_{\lambda_d} \to 0$, and when $s_2 \to 0$, $V_\lambda \to V_{\lambda_d}$, i.e., $V_\lambda \to 0$.
3) It is known from (70) that all closed-loop signals, including the sliding surfaces s_i $(i = 1, 2)$, and tracking error of the first-order filter μ_i $(i = 1, 2, 3)$, are all bounded. ■

IV. NUMERICAL SIMULATIONS

The performance of the proposed TABLF-based impact angle control guidance law (referenced as TABLFGL hereinafter) is fully testified by numerical simulations and performance comparison in this section.

A. CONSTANT VELOCITY MISSILE MODEL

In this subsection, it is assumed that the missile has a constant velocity of 340m/s and attack a ground target 8000m away. The normal acceleration of the missile is constrained within 20g, where $g = 9.8\text{m/s}^2$ is the acceleration of gravity. For the proposed TABLFGL (51), its parameters used in the following cases are listed in Table. 1.

TABLE 1. Parameters of the proposed guidance law.

$\epsilon = 1$	$k_1 = 3$	$k_2 = 5$	$\beta = 0.1$
$\tau_1 = 0.01$	$\tau_2 = 0.01$	$\tau_3 = 0.01$	$\gamma = 10$

1) CASE 1: ATTACKING A STATIONARY TARGET WITH DIFFERENT IMPACT ANGLES

Under the constraint of leading angle $\kappa_{\max} = 60°$, the missile with initial flight path angle of 45° is assumed in this case to attack a stationary target with different impact angles of 0°, −30°, −60°, −90°, −120°, −150°, −180°. Under the TABLFGL, it is observed from Fig. 4(a)–(c) that the missile can precisely attack the intended target with prescribed impact angles while satisfying the FOV constraint, and the final missile distance and impact angles of all engagement scenarios are listed in Table. 2. It is should be noted that the desired impact angles of scenarios 0° and −180° is set as −0.1° and −179.9°, for fear of prematurely terminating the simulation for the missile height is less than zero. Due to the TABLF, the relative velocity perpendicular to the LOS V_λ is prevented from overstepping its boundary k_{b_1} as shown in Fig. 4(d), which further ensures that the leading angle is constrained within the given constraint of $\kappa_{\max} = 60°$ as depicted in Fig. 4(c). Moreover, V_λ and the normal acceleration command a_M, as shown in Fig. 4(e), are both forced to eventually approaches zero, thereby guaranteeing a precise attack and maximizing the warhead effect. Noting that the intended target is stationary in this case, the missile flight path angle is equal to the LOS angle at impact time according to the following equation [23]

$$\lambda(t_f) = \tan^{-1}\left(\frac{V_M \sin\theta_M(t_f) - V_T \sin\theta_T(t_f)}{V_M \cos\theta_M(t_f) - V_T \cos\theta_T(t_f)}\right) \quad (73)$$

which is in accord with Fig. 4(f). Fig. 4(g)–(l) show the curves of the sliding surfaces s_1, s_2 and the tracking errors of the first-order filters μ_1, μ_2, μ_3, and the adaptive estimation value $\hat{D}$.

TABLE 2. Final miss distances and impact angles of Case 1.

λ_d	0°	−30°	−60°	−90°	−120°	−150°	−180°
$R(t_f)$	0.07m	0.01m	0.02m	0.25m	0.33m	0.20m	0.30m
$\lambda(t_f)$	−0.1°	−30°	−60°	−90°	−120°	−150°	−179.9°

TABLE 3. Final miss distances and impact angles of Case 2.

$\kappa_{\max}$	40°	50°	60°	70°	80°
$R(t_f)$	0.29m	0.21m	0.18m	0.01m	0.31m
$\lambda(t_f)$	−89.9°	−90°	−90°	−90°	−90°

2) CASE 2: ATTACKING A MOVING TARGET WITH DIFFERENT FOV ANGLES

In this case, the missile with initial flight path angle of 25° is assumed to attack a non-maneuvering receding target with desired impact angle of −90° in the presence of maximum leading angle of 40°, 50°, 60°, 70° and 80°, respectively. The velocity of moving target is as 30m/s. It is observed from Fig. 5(a)–(c) that without violating the FOV constraint, the missile is also capable of precisely attacking the intended target with desired impact angle. The final missile distance and impact angles of all engagement scenarios are listed in Table. 3. Noting that the intended target is moving, the boundary of V_λ is not constant but time-varying according to the definition $k_{b_1} = V_T \sin(\theta_T - \lambda) - V_M \sin\kappa_{\max}$. In such case, V_λ is also restricted to not overstepping this time-varying boundary and eventually forced to

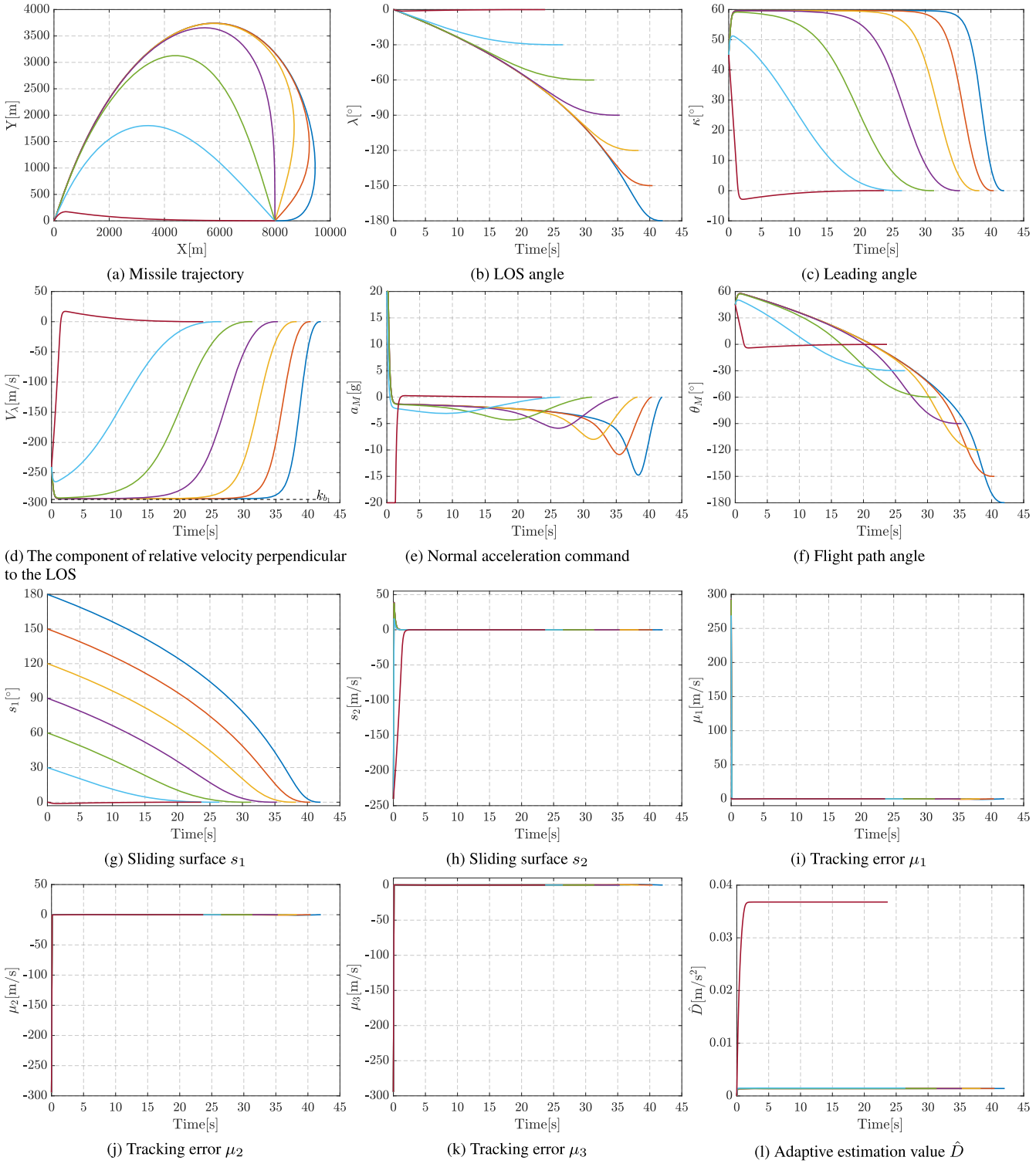

(a) Missile trajectory (b) LOS angle (c) Leading angle

(d) The component of relative velocity perpendicular to the LOS (e) Normal acceleration command (f) Flight path angle

(g) Sliding surface s_1 (h) Sliding surface s_2 (i) Tracking error μ_1

(j) Tracking error μ_2 (k) Tracking error μ_3 (l) Adaptive estimation value $\hat{D}$

FIGURE 4. Simulation results of attacking a stationary target with different impact angles.

approach zero as shown in Fig. 5(d), thereby satisfying the FOV constraint. It is to be noted that, according to

$$\begin{aligned} V_\lambda &= V_T \sin(\theta_T - \lambda) - V_M \sin(\theta_M - \lambda) \\ &= -V_T \sin\lambda - V_M \sin\kappa \end{aligned} \tag{74}$$

the leading angle is not equal to zero at impact time for the velocity of the target is not zero, as depicted in Fig. 5(c). For the same reason, it is observed from Fig. 5(f) that the missile flight path angle is not equal to the LOS angle at impact time yet, according to (73).

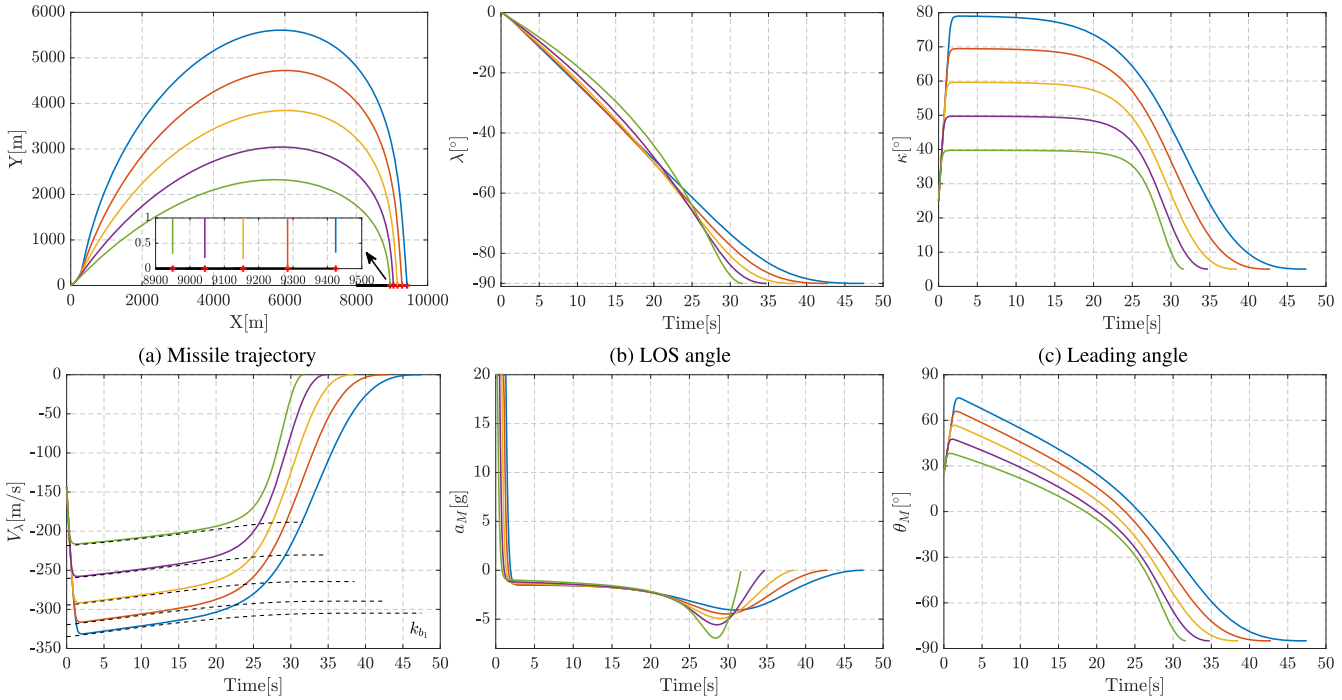

(a) Missile trajectory (b) LOS angle (c) Leading angle

(d) The component of relative velocity perpendicular to the LOS (e) Normal acceleration command (f) Flight path angle

FIGURE 5. Simulation results of attacking a moving target with different FOV angles.

B. VARYING VELOCITY MISSILE MODEL

This subsection considers a more realistic missile model, which is borrowed from [30] as

$$\begin{cases} \dot{x} = V_M \cos\theta_M \\ \dot{y} = V_M \sin\theta_M \\ \dot{V}_M = \dfrac{T-D}{m} - g\sin\theta_M \\ \dot{\theta}_M = \dfrac{a_M - g\cos\theta_M}{V_M} \end{cases} \tag{75}$$

where x, y denote the missile position with respect to the inertial coordinate system. The mass m and the thrust T are modeled as piecewise functions with respect to the time t as

$$m = \begin{cases} 135 - 14.53t, & 0 \le t < 1.5 \\ 113.205 - 3.31t, & 1.5 \le t < 8.5 \\ 90.035, & 8.5 \le t \end{cases} \tag{76}$$

$$T = \begin{cases} 33000, & 0 \le t < 1.5 \\ 7500, & 1.5 \le t < 8.5 \\ 0, & 8.5 \le t \end{cases} \tag{77}$$

The aerodynamic drag D is modeled as

$$\begin{cases} D = D_0 + D_i \\ D_0 = C_{d_0} QS \\ D_i = \dfrac{C_{d_i} m^2 a_M^2}{QS} \end{cases} \tag{78}$$

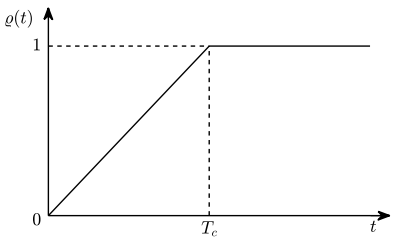

FIGURE 6. The configuration of BPNG.

where D_0 and D_i denote the zero-lift drag and induced drag, respectively. Their coefficients C_{d_0} and C_{d_i} are approximately modeled as piecewise functions with respect to the Mach number M_a as

$$C_{d_0} = \begin{cases} 0.02, & M_a < 0.93 \\ 0.02 + 0.2\,(M_a - 0.93)\,, & M_a < 1.03 \\ 0.04 + 0.06\,(M_a - 1.03)\,, & M_a < 1.10 \\ 0.0442 - 0.007\,(M_a - 1.10)\,, & M_a \ge 1.10 \end{cases} \tag{79}$$

$$C_{d_i} = \begin{cases} 0.2, & M_a < 1.15 \\ 0.2 + 0.246\,(M_a - 1.15)\,, & M_a \ge 1.15 \end{cases} \tag{80}$$

where $Q = \dfrac{1}{2}\rho V_M^2$ is the dynamic pressure, $S = 1$ is the reference area. The atmosphere density ρ below the height of 20000m is given by

$$\rho(y) = 1.15579 - 1.058 \times 10^{-4} y + 3.725 \times 10^{-9} y^2 - 6.0 \times 10^{-14} y^3 \tag{81}$$

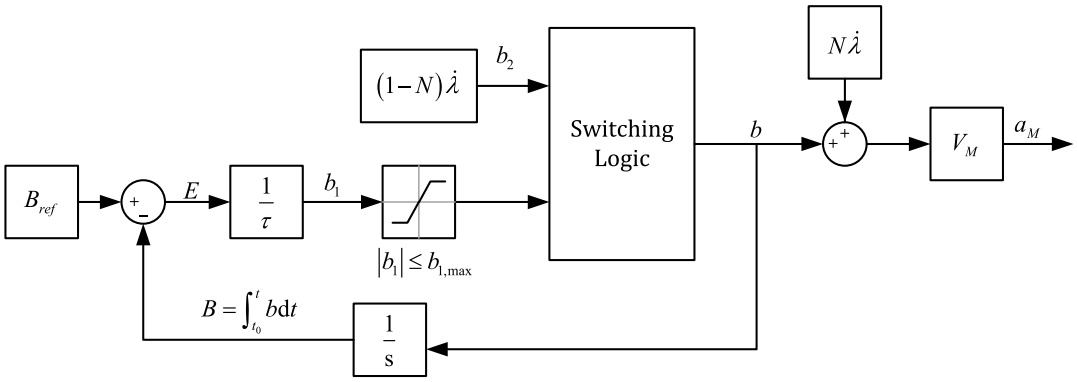

FIGURE 7. The graph of correction function $\varrho(t)$.

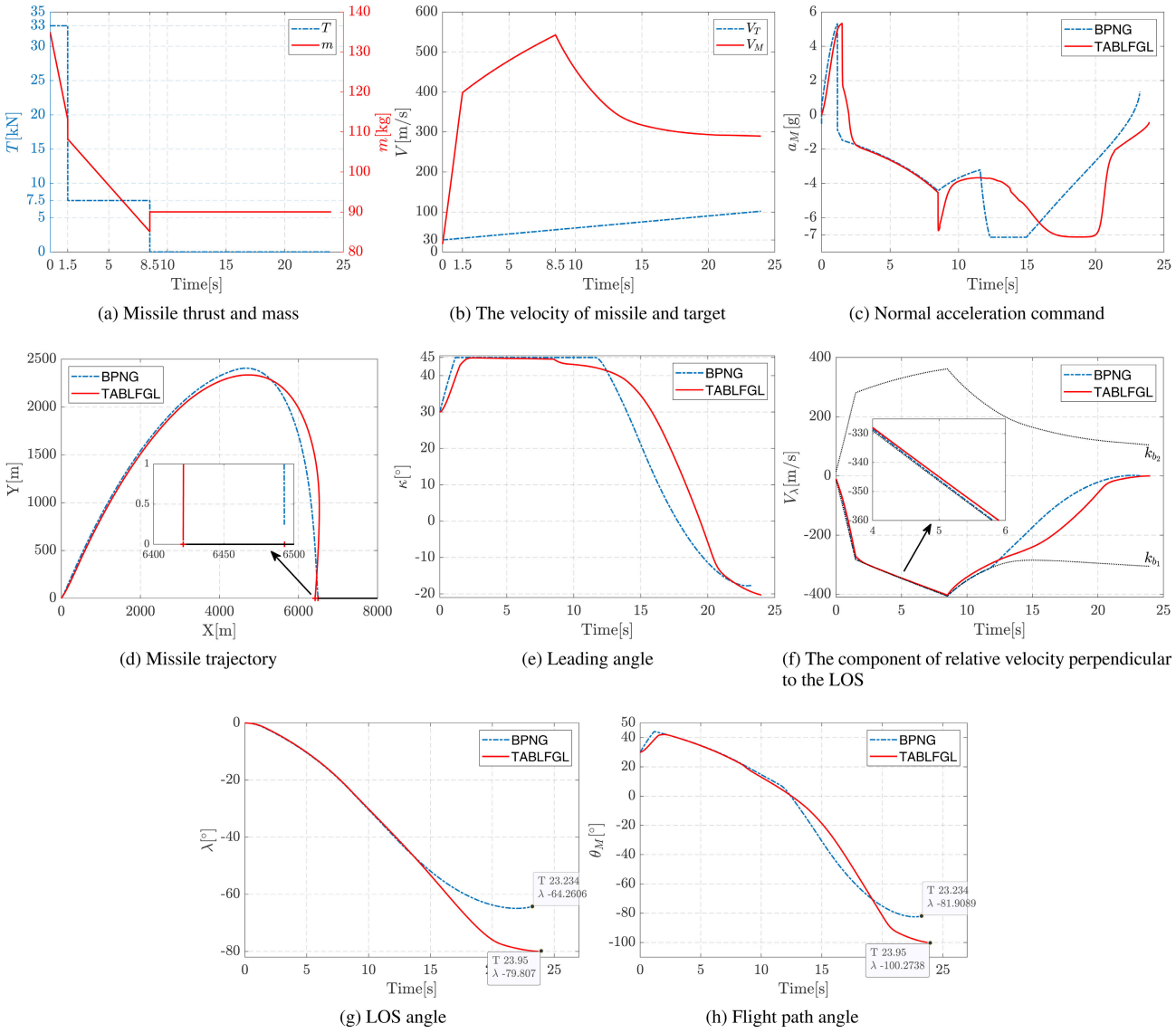

(a) Missile thrust and mass
(b) The velocity of missile and target
(c) Normal acceleration command
(d) Missile trajectory
(e) Leading angle
(f) The component of relative velocity perpendicular to the LOS
(g) LOS angle
(h) Flight path angle

FIGURE 8. Comparative simulation results of attacking a maneuvering approaching target.

The normal acceleration command of the proposed guidance law is always saturated at initial phase, but the induced drag of the realistic missile model (75) is proportional to the square of normal acceleration. For fear of prematurely terminating the simulation caused by $T \ll D$ at the begin, the normal acceleration command (43) is

modified as

$$a^*_{M_c} = \varrho(t) a_{M_c} \tag{82}$$

where $\varrho(t)$ is a correction function and its graph is shown in Fig. 7

$$\varrho(t) = \begin{cases} 1 - \left(\dfrac{T_c - t}{T_c}\right)^{\varsigma}, & t \le T_c \\ 1, & t > T_c \end{cases} \tag{83}$$

where ς is a positive constant.

This subsection compares the TABLFGL with a bias-shaping proportional navigation guidance law (BPNG) [23], which is summarized $a_{M_c} = V_M\left(N\dot{\lambda} + b\right)$, where

$$b = \begin{cases} b_1 = \dfrac{B_{ref}}{\tau} \mathrm{e}^{-\frac{t}{\tau}}, & \text{for the initial homing phase} \\ b_2 = (1-N)\,\dot{\lambda}, & \text{if } |\kappa(t)| \ge \kappa_{\max} \\ b_1 = \dfrac{B_{ref}}{\tau} \mathrm{e}^{-\frac{t}{\tau}}, & \text{if } |b_1(t)| \le |b_2(t)| \text{ until interception} \end{cases} \tag{84}$$

where navigation gain $N \ge 2\,(1 + V_T/V_M)$ and design parameter $\tau > 0$. The desired integral value of bias satisfies

$$B_{ref} = \theta_M(t_f) - \theta_M(t_0) - N \tan^{-1}\left(\frac{V_M \sin\theta_M(t_f)}{V_M \cos\theta_M(t_f) - V_T \cos\theta_T}\right) \tag{85}$$

The configuration of BPNG is depicted in Fig. 6.

Under the proposed and comparative guidance laws, the missile with initial velocity of 20m/s and initial flight path angle of 30° is assumed to attack a maneuvering approaching target 8000m away with the desired impact angle of −80°. The maximum leading angle of the missile is $\kappa_{\max} = 45°$, and the limit of missile normal acceleration is given by $80\mathrm{m/s}^2$. The acceleration of the moving target with 30m/s initial velocity is $3\mathrm{m/s}^2$. Under the guidance parameter listed in Table. 4, the simulation result is shown in Fig. 8.

TABLE 4. Parameters of TABLFGL and BPNG.

The guidance parameter of TABLFGL				
$\epsilon = 3$ $\tau_1 = 0.01$	$k_1 = 3$ $\tau_2 = 0.01$	$k_2 = 5$ $\tau_3 = 0.01$	$\beta = 1$ $\gamma = 2$	$T_c = 2$ $\varsigma = 0.2$
The guidance parameter of BPNG				
$\tau = 1$	$N = 3$			

It is clear from Fig. 8(a) that both the thrust and mass of missile model are discontinuous, thus leading to obvious sharp corners in curves of missile velocity and normal acceleration as shown in Fig. 8(b)–(c). Also, it can be observed from Fig. 8(c) that the normal acceleration commands of TABLFGL and BPNG are both saturated for the maneuvering movement of the approaching target. In addition, it is noticed that the normal acceleration command of TABLFGL can approach zero at impact time but the one under BPNG cannot, which would cause the ricochet phenomenon due to nonzero angle of attack. From Fig. 8(d)–(e), it is observed that both the two guidance laws can steer the missile to the intended target with a satisfactory miss distance of less than 0.5m, while satisfying the FOV constraint. It is the flight path angle at impact time that is defined as the desired impact angle for BPNG. It is therefore concluded from Fig. 8(g)–(h) that the objective of impact angle control for the two guidance laws are both achieve, despite a larger error of the BPNG. It is worth noting that the precise information required for calculating B_{ref} (85) is assumed to be available when implementing simulations. If an average speed of about Mach 0.7 and initial target velocity, according to Park [23], are used to compute B_{ref} off-line, there is an unacceptable impact angle error of up to 20° as shown in Fig. 9.

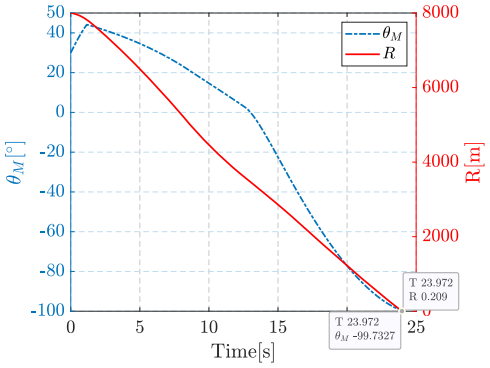

FIGURE 9. Simulation results of BPNG with B_{ref} calculated off-line.

V. CONCLUSION

In this article, a novel impact angle control guidance law against stationary and moving target is proposed to address the problem of FOV constraint. The FOV constraint imposed on the BLOS angle is transformed to a time-varying asymmetric limitation of the relative velocity perpendicular to the LOS between missile and target. Based on the dynamic surface control and time-varying asymmetric BLF, this relative velocity under the proposed guidance law is prevented from overstepping the time-varying asymmetric limitation and eventually approach zero, thus satisfying the homing requirement without violating the FOV constraint. The performance of the proposed guidance law is fully demonstrated by extensive numerical simulations and performance comparison.

APPENDIX
PROOF OF LEMMA 3

Proof: Letting $x = \dfrac{s}{k}$, the aforementioned proposition can be equally transformed to: for $\forall\,|x| < 1$, the following inequality holds

$$x^2 \le \log\frac{1}{1-x^2} \le \frac{x^2}{1-x^2} \tag{86}$$

where the equal sign holds if and only if $x = 0$.

Prove the inequality on the right side first.

Define the function

$$f(x) = \log \frac{1}{1-x^2} - \frac{x^2}{1-x^2} \tag{87}$$

Its derivative function is

$$f'(x) = (1-x^2)\frac{2x}{(1-x^2)^2} - \frac{2x(1-x^2)+x^2\cdot 2x}{(1-x^2)^2} = \frac{-2x^3}{(1-x^2)^2} \tag{88}$$

When $-1 < x < 0, f'(x) > 0, f(x)$ is a increasing function, and when $0 < x < 1, f'(x) < 0, f(x)$ is a decreasing function. When $x = 0, f'(x) = 0, f(x)$ takes the maximum value in the domain $(-1, 1), f(0) = 0$. That is, for $\forall |x| < 1$, $f(x) \leq 0$, namely

$$\log \frac{1}{1-x^2} \leq \frac{x^2}{1-x^2} \tag{89}$$

where the equal sign holds if and only if $x = 0$.

Then prove the inequality on the left side.

Define the function

$$f(x) = \log \frac{1}{1-x^2} - x^2 \tag{90}$$

Its derivative function is

$$f'(x) = (1-x^2)\frac{2x}{(1-x^2)^2} - 2x = \frac{2x^3}{1-x^2} \tag{91}$$

When $-1 < x < 0, f'(x) < 0, f(x)$ is a decreasing function, and when $0 < x < 1, f'(x) > 0, f(x)$ is a increasing function. When $x = 0, f'(x) = 0, f(x)$ takes the minimum value in the domain $(-1, 1), f(0) = 0$. That is, for $\forall |x| < 1$, $f(x) \geq 0$, namely

$$\log \frac{1}{1-x^2} \geq x^2 \tag{92}$$

where the equal sign holds if and only if $x = 0$. ■

REFERENCES

[1] R. Tekin and K. S. Erer, "Switched-gain guidance for impact angle control under physical constraints," *J. Guid., Control, Dyn.*, vol. 38, no. 2, pp. 205–216, Feb. 2015.

[2] B. Soo Kim, J. Gyu Lee, and H. Seok Han, "Biased PNG law for impact with angular constraint," *IEEE Trans. Aerosp. Electron. Syst.*, vol. 34, no. 1, pp. 277–288, Jan. 1998.

[3] A. Ratnoo and D. Ghose, "Impact angle constrained interception of stationary targets," *J. Guid., Control, Dyn.*, vol. 31, no. 6, pp. 1816–1821, Nov. 2008.

[4] A. Ratnoo and D. Ghose, "Impact angle constrained guidance against nonstationary nonmaneuvering targets," *J. Guid., Control, Dyn.*, vol. 33, no. 1, pp. 269–275, Jan. 2010.

[5] K. S. Erer and O. Merttopçuoglu, "Indirect impact-angle-control against stationary targets using biased pure proportional navigation," *J. Guid., Control, Dyn.*, vol. 35, no. 2, pp. 700–703, 2012.

[6] A. Ratnoo, "Nonswitching guidance law for trajectory shaping control," *J. Guid., Control, Dyn.*, vol. 40, no. 10, pp. 2717–2724, 2017.

[7] V. Shaferman and T. Shima, "Linear quadratic guidance laws for imposing a terminal intercept angle," *J. Guid., Control, Dyn.*, vol. 31, no. 5, pp. 1400–1412, Sep. 2008.

[8] H.-S. Shin, J.-I. Lee, A. Tsourdos, and M.-J. Tahk, "Homing guidance law for reducing sensitivity on heading error," in *Proc. AIAA Guid., Navigat., Control Conf.* Minneapolis, MI, USA: AIAA, Aug. 2012, pp. 1–16.

[9] C.-H. Lee, J.-I. Lee, and M.-J. Tahk, "Sinusoidal function weighted optimal guidance laws," *Proc. Inst. Mech. Eng., G, J. Aerosp. Eng.*, vol. 229, no. 3, pp. 534–542, Mar. 2015.

[10] J.-I. Lee, I.-S. Jeon, and C.-H. Lee, "Command-shaping guidance law based on a Gaussian weighting function," *IEEE Trans. Aerosp. Electron. Syst.*, vol. 50, no. 1, pp. 772–777, Jan. 2014.

[11] C.-K. Ryoo, H. Cho, and M.-J. Tahk, "Time-to-go weighted optimal guidance with impact angle constraints," *IEEE Trans. Control Syst. Technol.*, vol. 14, no. 3, pp. 1562–1572, Apr. 2006.

[12] J. Z. Ben-Asher, N. Farber, and S. Levinson, "New proportional navigation law for ground-to-air systems," *J. Guid., Control, Dyn.*, vol. 26, no. 5, pp. 822–825, Sep. 2003.

[13] C.-H. Lee and M.-G. Seo, "New insights into guidance laws with terminal angle constraints," *J. Guid., Control, Dyn.*, vol. 41, no. 8, pp. 1828–1833, 2018.

[14] M. Xin, S. Balakrishnan, and E. Ohlmeyer, "Guidance law design for missiles with reduced seeker field-of-view," in *Proc. AIAA Guid., Navigat., Control Conf. Exhib.* Keystone, CO, USA: AIAA, Aug. 2006, p. 6085.

[15] B.-G. Park, T.-H. Kim, and M.-J. Tahk, "Optimal impact angle control guidance law considering the seeker's field-of-view limits," *Proc. Inst. Mech. Eng., G, J. Aerosp. Eng.*, vol. 227, no. 8, pp. 1347–1364, Jun. 2013.

[16] B.-G. Park, T.-H. Kim, and M.-J. Tahk, "Range-to-go weighted optimal guidance with impact angle constraint and seeker's look angle limits," *IEEE Trans. Aerosp. Electron. Syst.*, vol. 52, no. 3, pp. 1241–1256, Jun. 2016.

[17] C.-H. Lee, T.-H. Kim, M.-J. Tahk, and I.-H. Whang, "Polynomial guidance laws considering terminal impact angle and acceleration constraints," *IEEE Trans. Aerosp. Electron. Syst.*, vol. 49, no. 1, pp. 74–92, Jan. 2013.

[18] L. Ran, W. Qiuqiu, T. Wangchun, and Z. Yijie, "Adaptive weighting impact angle optimal guidance law considering seeker's FOV angle constraints," *J. Syst. Eng. Electron.*, vol. 29, no. 1, pp. 142–151, Feb. 2018.

[19] B.-G. Park, B.-J. Jeon, T.-H. Kim, M.-J. Tahk, and Y.-H. Kim, "Composite guidance law for impact angle control of tactical missiles with passive seekers," in *Proc. Asia–Pacific Int. Symp. Aerosp. Technol.* Seoul, South Korea: The Korean Society for Aeronautical & Space Sciences, 2012, pp. 13–15.

[20] B.-G. Park, H.-H. Kwon, Y.-H. Kim, and T.-H. Kim, "Composite guidance scheme for impact angle control against a nonmaneuvering moving target," *J. Guid., Control Dyn.*, vol. 39, no. 5, pp. 1129–1136, May 2016.

[21] A. Ratnoo, "Analysis of two-stage proportional navigation with heading constraints," *J. Guid., Control, Dyn.*, vol. 39, no. 1, pp. 156–164, Jan. 2016.

[22] T.-H. Kim, B.-G. Park, and M.-J. Tahk, "Bias-shaping method for biased proportional navigation with terminal-angle constraint," *J. Guid., Control, Dyn.*, vol. 36, no. 6, pp. 1810–1815, 2013.

[23] B.-G. Park, T.-H. Kim, and M.-J. Tahk, "Biased PNG with terminal-angle constraint for intercepting nonmaneuvering targets under physical constraints," *IEEE Trans. Aerosp. Electron. Syst.*, vol. 53, no. 3, pp. 1562–1572, Jun. 2017.

[24] Y.-I. Lee, S.-H. Kim, and M.-J. Tahk, "Optimality of linear time-varying guidance for impact angle control," *IEEE Trans. Aerosp. Electron. Syst.*, vol. 48, no. 4, pp. 2802–2817, Oct. 2012.

[25] X. Wang, Y. Zhang, and H. Wu, "Sliding mode control based impact angle control guidance considering the seeker's field-of-view constraint," *ISA Trans.*, vol. 61, pp. 49–59, Mar. 2016.

[26] B. Liu, M. Hou, and D. Feng, "Nonlinear mapping based impact angle control guidance with seeker's field-of-view constraint," *Aerosp. Sci. Technol.*, vol. 86, pp. 724–736, Mar. 2019.

[27] K. P. Tee, S. S. Ge, and E. H. Tay, "Barrier Lyapunov functions for the control of output-constrained nonlinear systems," *Automatica*, vol. 45, no. 4, pp. 918–927, Apr. 2009.

[28] Y. He, C. Lu, J. Shen, and C. Yuan, "Design and analysis of output feedback constraint control for antilock braking system with time-varying slip ratio," *Math. Problems Eng.*, vol. 2019, Jan. 2019, Art. no. 8193134.

[29] W. Wang, S. Xiong, S. Wang, S. Song, and C. Lai, "Three dimensional impact angle constrained integrated guidance and control for missiles with input saturation and actuator failure," *Aerosp. Sci. Technol.*, vol. 53, pp. 169–187, Jun. 2016.

[30] P. Kee, L. Dong, and C. Siong, "Near optimal midcourse guidance law for flight vehicle," in *Proc. 36th AIAA Aerosp. Sci. Meeting Exhib.* Reno, NV, USA: AIAA, Jan. 1998, pp. 1–11.

JIAYI TIAN received the B.S. degree in aircraft design from Beihang University, Beijing, China, in 2013, and the M.S. and Ph.D. degrees in aeronautical and astronautical science and technology from the National University of Defense Technology, Changsha, China, in 2015 and 2019, respectively. Since 2020, he has been an Engineer with the China Aerodynamics Research and Development Center, Mianyang, China. His research interests include disturbance rejection-based control and aircraft dynamics and control.

XIBIN BAI received the B.S. degree in space engineering and the M.S. and Ph.D. degrees in aeronautical and astronautical science and technology from the National University of Defense Technology, Changsha, China, in 2011, 2013, and 2018, respectively. Since 2019, he has been a Lecturer with the National University of Defense Technology. His research interests include inertial navigation and aircraft dynamics and control.

HUABO YANG received the Ph.D. degree in aircraft design from the National University of Defense Technology, Changsha, China, in 2008. In 2013, he was appointed as an Associate Professor at the College of Aeronautics and Astronautics, National University of Defense Technology. His research interests include test and calibration of inertial measurement unit, flight dynamics, and guidance and control.

SHIFENG ZHANG received the Ph.D. degree in control theory and engineering from the National University of Defense Technology, Changsha, China, in 2000. Since 2010, he has been a Professor and a Ph.D. Supervisor with the College of Aeronautics and Astronautics, National University of Defense Technology. His research interests include aircraft overall design, flight dynamics, guidance and control, inertial navigation, and measurement and precision analysis.